A LETTERS JOURNAL EXPLORING THE FRONTIERS OF PHYSICS

OFFPRINT

Phase space distribution of an electron beam emerging from Compton/Thomson back-scattering by an intense laser pulse

V. Petrillo, I. Chaikovska, C. Ronsivalle, A. R. Rossi, L. Serafini and C. Vaccarezza

EPL, **101** (2013) 10008

epl

A Letters Journal Exploring the Frontiers of Physics

AN INVITATION TO SUBMIT YOUR WORK

www.epljournal.org

The Editorial Board invites you to submit your letters to EPL

EPL is a leading international journal publishing original, high-quality Letters in all areas of physics, ranging from condensed matter topics and interdisciplinary research to astrophysics, geophysics, plasma and fusion sciences, including those with application potential.

The high profile of the journal combined with the excellent scientific quality of the articles continue to ensure EPL is an essential resource for its worldwide audience. EPL offers authors global visibility and a great opportunity to share their work with others across the whole of the physics community.

Run by active scientists, for scientists

EPL is reviewed by scientists for scientists, to serve and support the international scientific community. The Editorial Board is a team of active research scientists with an expert understanding of the needs of both authors and researchers.

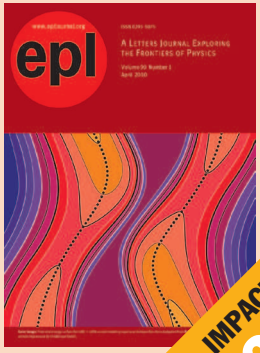

IMPACT FACTOR 2.753*

*As ranked by ISI 2010

IMPACT FACTOR
2.753*
* As listed in the ISI® 2010 Science Citation Index Journal Citation Reports

OVER
500 000
full text downloads in 2010

30 DAYS
average receipt to online publication in 2010

16 961
citations in 2010
37% increase from 2007

"We've had a very positive experience with EPL, and not only on this occasion. The fact that one can identify an appropriate editor, and the editor is an active scientist in the field, makes a huge difference."

Dr. Ivar Martinv
Los Alamos National Laboratory, USA

Six good reasons to publish with EPL

We want to work with you to help gain recognition for your high-quality work through worldwide visibility and high citations.

1. **Quality** – The 40+ Co-Editors, who are experts in their fields, oversee the entire peer-review process, from selection of the referees to making all final acceptance decisions
2. **Impact Factor** – The 2010 Impact Factor is 2.753; your work will be in the right place to be cited by your peers
3. **Speed of processing** – We aim to provide you with a quick and efficient service; the median time from acceptance to online publication is 30 days
4. **High visibility** – All articles are free to read for 30 days from online publication date
5. **International reach** – Over 2,000 institutions have access to EPL, enabling your work to be read by your peers in 100 countries
6. **Open Access** – Articles are offered open access for a one-off author payment

Details on preparing, submitting and tracking the progress of your manuscript from submission to acceptance are available on the EPL submission website **www.epletters.net**.

If you would like further information about our author service or EPL in general, please visit **www.epljournal.org** or e-mail us at **info@epljournal.org**.

EPL is published in partnership with:

European Physical Society | Società Italiana di Fisica | EDP Sciences | IOP Publishing

A Letters Journal Exploring the Frontiers of Physics

January 2013

EPL, **101** (2013) 10008
doi: 10.1209/0295-5075/101/10008

www.epljournal.org

Phase space distribution of an electron beam emerging from Compton/Thomson back-scattering by an intense laser pulse

V. Petrillo[1], I. Chaikovska[2], C. Ronsivalle[3], A. R. Rossi[1], L. Serafini[1] and C. Vaccarezza[4(a)]

[1] *INFN, Università degli Studi Milano - Via Celoria, 16, 20133 Milano, Italy, EU*
[2] *LAL, Université Paris-Sud, IN2P3/CNRS - Orsay-Ville, France, EU*
[3] *ENEA - Via E. Fermi, 45, Frascati (Rm), Italy, EU*
[4] *INFN-LNF Via E. Fermi, 40, Frascati (Rm), Italy, EU*

received 14 November 2012; accepted in final form 16 December 2012
published online 21 January 2013

PACS 03.65.Nk – Scattering theory
PACS 41.60.Cr – Free-electron lasers

Abstract – We analyze the energy distribution of a relativistic electron beam after the Compton back-scattering by a counterpropagating laser field. The analysis is performed for parameters in the range of realistic X-γ sources, in the framework of the Quantum Electrodynamics, by means of the code CAIN. The results lead to the conclusion that, in the regime considered, the main effect is the initial formation of stripes, followed by the diffusion of the most energetic particles toward lower values in the longitudinal phase space, with a final increase of the electron energy bandwidth.

The distribution in the phase space of the electrons after the Thomson/Compton back-scattering by a laser pulse has been object of recent discussions. In refs. [1,2], the authors revisited the theoretical model that provides the electron energy distribution evolution during the emission of radiation by relativistic electrons entering an undulating field. They claimed that a drift-diffusion approach, such as that proposed in [3,4], is not sufficient to describe the phenomenon over the entire range of the parameters and that a previously unknown quantum effect occurs and persists in time when the parameter $\epsilon = N_w \hbar\omega/(\gamma mc^2)$ is of the order of or larger than unity, where N_w is the number of undulator field periods for the case of undulator radiation or the number of oscillations of the laser field for the case of Thomson/Compton scattering, $\hbar$ is the reduced Planck constant, ω is the photon frequency, γ the relativistic Lorentz factor, m the electron rest mass and c the speed of light. They proposed to adopt a finite-difference equation with a fix momentum exchange for modeling the electron distribution. The results should be a relevant deformation of the electron energy distribution associated with spontaneous emission in long undulators, that should present a sequence of regular lines, which reveal discrete momentum groups in accord with a Poisson distribution. It should be noted that the previous model neglects the angle-frequency correlation of the spontaneously emitted radiation and, as a consequence, underestimates the natural bandwidth, because it assumes the emission of photons wiht a well-defined momentum $\hbar k$, a radiation linewidth given by $\Delta\omega/\omega \sim 1/N_w$, and a corresponding uncertainty in the photon momentum $\hbar\Delta k \sim \hbar k N_w$.

A strong objection has been formulated in [5,6] where the authors argued that the angular distribution of the radiation was completely disregarded in ref. [1], the model being one-dimensional and the spontaneous emission being considered only on axis, *i.e.*, for an emission angle much smaller than $1/\gamma$. Neglecting angular and inhomogeneous effects, the overall relative bandwidth results to be due only to the length of the undulating field, *i.e.*, of the order of $1/N_w$. On the contrary, the electron recoil and, in turn, the electron distribution after the collision, depend on the entire angular distribution of the radiation, which is a fundamental feature of the Compton/Thomson effects. When the angular distribution of the radiation is properly accounted for, the overall angle-integrated relative bandwidth results to be independent of the number of undulator periods and is dominated by the acceptance, as well as the by the emittance and energy spread of the electron beam, the frequency bandwidth and diffraction of the laser across the interaction focal area. The conclusions exposed in refs. [5,6] are that a three-dimensional drift-diffusion

(a) E-mail: petrillo@mi.infn.it

model is valid for large times (*i.e.*, for $N_w \gg 1$) and when the parameter $\zeta = \hbar\omega/(\gamma mc^2)$, which is a factor N_w smaller than ϵ, is much smaller than unity. A Fokker-Planck approach covers, therefore, all cases of practical interest. Similar conclusions are presented in [7], where continuous electron distributions, which are the solution of a master equation derived from the Chapman-Kolmogorov equation for Markov phenomena with the Compton transition probability [8], are shown.

Our contribution to the debate is based on a different philosophy. We present in fact numerical calculations of the head-on Thomson/Compton inverse scattering performed with the well-known code CAIN [9,10], obtained by using ideal and simulated beams with parameters covering the range of realistic X and γ sources, as for instance PlasmonX [11] at SparcLab [12] and ELI-NP [13]. We will show in this letter that the time evolution of the electron energy distribution during a Compton back-scattering, as far as the kinematics of the interaction is described by electron-photon collisions, presents an initial phase with a gradual population of stripes at lower energies, with a subsequent drain, followed by a regime of standard diffusion. We will show, furthermore, that the rearrangement of the electrons in the phase space is ascribable to a random walk with non-uniform step, similar to that described in ref. [14], that the initial, non-classical phase is merely due to the two-bodies model adopted for the kinematic of the collision and to the relativistic resonant character of the cross-section, and that the diffusion regime is achieved when $\zeta \ll 1$ and the average number of emitted photons per electron during the whole interaction is larger than one. We can conclude therefore that the Thomson/Compton scattering does not lead to the formation of quantum lines and that, in the initial phase, there is trace of the quantum nature of the phenomenon in the occurrence of the stripes, while at long times, the establishment of a diffusive regime can be observed, according to what reported in refs. [5,7].

The code CAIN, used in the simulations, is based on a Monte Carlo procedure that randomly selects couples of colliding particles among the electron and laser beams, the probability of the Thomson/Compton back-scattering being weighted by the Klein-Nishina cross-section obtained with a standard QED calculation. The code has been widely benchmarked for the electron-photon interaction by experimental data [15] and by analytical models [15,16]. Starting with the complete initial phase spaces of both colliding beams in the interaction point, it provides the whole phase spaces after the scattering. It works with both the linear and the non-linear cross-section.

The first case we have analyzed is the X Thomson source PlasmonX [11] at Sparc-Lab [12], operated at 150 MeV. The electron beam, whose parameters are in table 1, beam A, collides with the Ti:Sapphire Laser FLAME [17], with wavelength $\lambda_L = 2\pi c/\omega_L = 800$ nm and whose nominal energy E_L can reach 5 J.

Table 1: Electron beam and laser pulse main characteristics.

Quantity	(A)	(B)	(C)
Charge (pC)	250	250	250
Energy (MeV)	150	360	360
Energy spread (MeV)	–	–	0.234
x emittance (mm mrad)	1	0.5	0.65
y emittance (mm mrad)	1	0.5	0.6
Laser wavelength (nm)	800	500	500
Laser energy (J)	< 3	1–16	1
Laser r.m.s. time duration (ps)	0.08–10	6–96	5
Maximum photon energy (MeV)	0.5	4.9	4.9
Quantum red shift (keV)	2	6.7	6.7

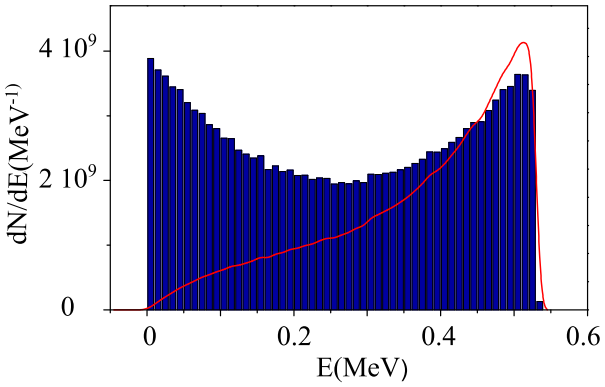

Fig. 1: (Colour on-line) Photon distribution $\mathrm{d}N/\mathrm{d}E$ (MeV^{-1}) *vs.* energy E in MeV for the parameters of table 1 (A) and the laser parameter $a_0 = 0.05$. On the left axis: navy columns: complete spectrum. On the right axis: red line: energy spectrum of the radiation in arbitrary units.

Photons up to 500 keV of energy are produced, whose distribution in number and energy is presented in fig. 1. The radiation emitted in the scattering is characterized by the broadband spectrum typical of the Thomson/Compton interaction. As can be seen, the amount of photons emitted with an energy lower than the nominal resonance value on axis,

$$E_r = \hbar\omega \approx \frac{\hbar\omega_L(1+\beta_z)}{(1-\beta_z+2\hbar\omega_L/mc^2\gamma)}, \qquad (1)$$

is very important, leading to an energy spectrum $\mathrm{d}W/\mathrm{d}E$ (fig. 1, red curve) with average value $\langle E\rangle = 372.5$ keV, r.m.s. value $E_{\mathrm{rms}} = \sqrt{\langle (E-\langle E\rangle)^2\rangle} = 177.5$ keV, and relative bandwidth larger than 37%. Low laser energy densities have been considered, in order to avoid non-linear effects which enlarge the bandwidth towards higher values. A first criterion for weighting the occurrence of quantum effects is the importance of the quantum recoil. If the condition $2\hbar\omega_L/mc^2 \ll 1/\gamma$ is satisfied, the red shift in (1) due to the electron recoil can be neglected and the classical regime is retrieved. In the present case the quantum red shift is 2 keV, a value much lower than the average photon energy. Radiations with thinner bandwidth, suitable for applications, can be obtained by inserting irides or collimators

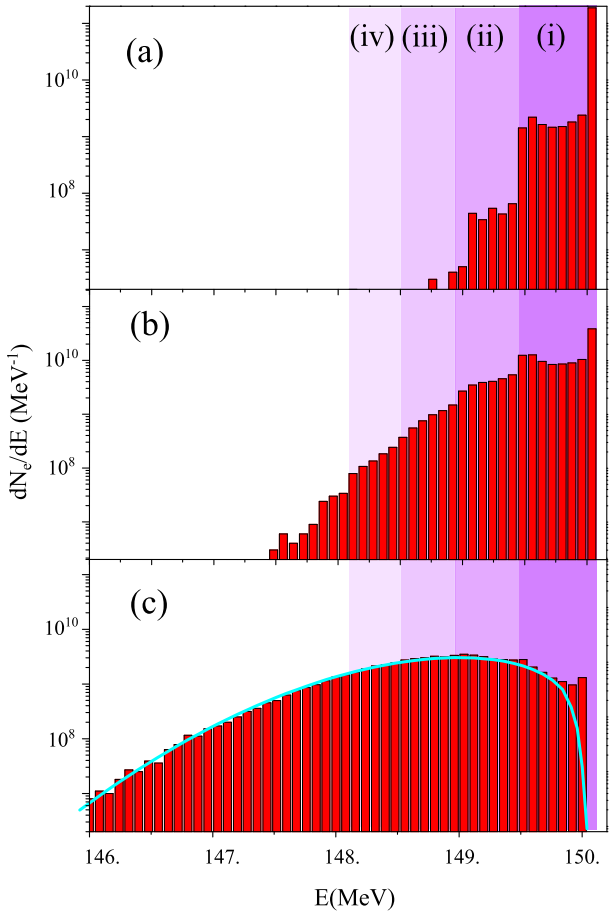

Fig. 2: (Colour on-line) Electron distribution $\mathrm{d}N_e/\mathrm{d}E(\mathrm{MeV}^{-1})$ *vs.* electron energy in MeV for the case without diffraction (Rayleigh length $L_R = 10\,\mathrm{mm}$) and for $a_0 = 0.083$. (a) $\Delta t = 0.083\,\mathrm{ps}$, $E_L = 1\,\mathrm{J}$ ($F_X = 0.0145$); (b) $\Delta t = 1.66\,\mathrm{ps}$, $E_L = 20\,\mathrm{J}$ ($F_X = 0.29$); (c) $\Delta t = 6.66\,\mathrm{ps}$, $E_L = 80\,\mathrm{J}$ ($F_X = 1.16$). The curve in panel (c) represents the Rayleigh distribution function associated to random walk for $N = 4.5$.

along the radiation trajectory, taking advantage of the characteristic angle-frequency correlation, typical of the Thomson/Compton scattering [18,19].

The energy of the electrons, on the contrary, changes during the radiation emission due to the whole broadband spectrum and evolves in the longitudinal phase space in a way connected with the shape of the energy distribution of the radiation. The distribution of the electrons after the scattering is presented in fig. 2 for different values of the laser time duration at the same peak laser parameter $a_0 = \frac{eE_0}{mc\omega_L}$, where E_0 is the peak laser field. If the laser power is supposed to be Gaussian both in the transverse and in the longitudinal direction with r.m.s. dimensions given, respectively, by σ and $c\Delta t$, the laser parameter can be written as $a_0 = 1.5\frac{\lambda_L}{\sigma}\sqrt{\frac{E_L\,(\mathrm{J})}{\Delta t\,(\mathrm{ps})}}$ and, in our case, has the value $a_0 = 0.083$. The second parameter that rules the quantum character of the system is the number of emitted photons per electron, that in the quantum regime has to be much smaller than one. From a simple definition of the luminosity of the system [10],

$$L = \frac{N_L N_e}{2\pi(\sigma^2 + \sigma_e^2)}, \tag{2}$$

with $N_L = E_L/(\hbar\omega_L)$, N_e the total number of electrons and σ_e the transverse dimension of the electron beam, the number of emitted photons N can be introduced:

$$N = L\sigma_T, \tag{3}$$

where $\sigma_T = \frac{8}{3}r_e^2$ is the total Thomson cross-section, and r_e the classical electron radius. Finally, the number of emitted photons per electron is

$$F_X = \frac{N}{N_e} = \frac{E_L\sigma_T}{2\pi\hbar\omega_L(\sigma^2 + \sigma_e^2)}, \tag{4}$$

which, for the previous case, assumes values between $1.45\cdot10^{-2}$ and 1.16.

Starting from the case of shorter laser pulse (fig. 2(a)), the electron distribution develops a tail which is shaped in a complementary way with respect to the photon spectrum, thus forming a sort of plateau between 150 MeV and 149.5 MeV (zone (i)), with a flat peak in correspondence with the latter value (*i.e.*, 149.5 MeV), which is about 500 keV less than the Compton edge, due to this energy loss by most electrons in their first collision. Another low plateau appears below this value, down to 149 MeV (zone (ii)). It reveals the occurrence of cascaded emission from electrons that have already undergone a first scattering and that perform two successive collisions within $\Delta t = 0.083\,\mathrm{ps}$. Increasing the laser time duration (fig. 2(b) and (c)), these stripes become more populated, and a third zone, between 149 and 148.5 MeV, fills up by the electrons (zone (iii)) that participate to three collisions. Increasing further the time duration of the laser, the first zone begins to drain, the level of the lower stripes increases, then the differences between the zones disappear and the distribution overruns towards left and becomes smoother, similar to what happens in ref. [7]. In fig. 2(c), the Rayleigh distribution function associated to a diffusive process ruled by the random walk is also presented:

$$P_R(\delta E) \propto \frac{\delta E}{N}\, e^{-\frac{\delta E^2}{2N}}, \tag{5}$$

where $\delta E = |\frac{E-E_i}{E_r}|$, E_i is the electron energy before the collision and N is the number of steps. P_R begins to give a good representation of the energy distribution with a value of N a factor of four larger than F_X, apart from the first stripe. The difference between N and F_X, besides the fact that the diffusion regime is still at an early phase, depends on other factors, *i.e.*, the anisotropy of the random walk, the presence of space-time profiles in our model, the emittance of the electron beam. As regards the effect of the energy spread of the electron beam, values $\Delta E \ll \hbar\omega$ would permit to observe the formation of the stripes, corresponding to a relative energy

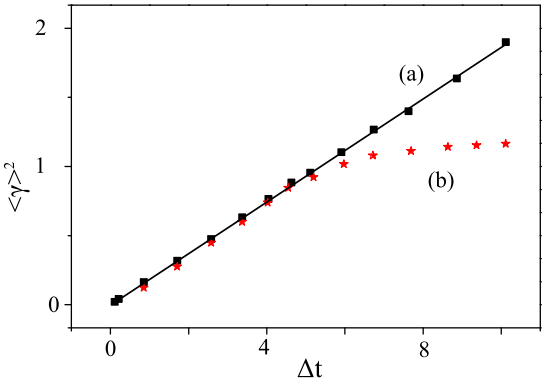

Fig. 3: (Colour on-line) $\langle\gamma^2\rangle$ *vs.* Δt for the case without diffraction (a) and with diffraction (b).

spread $\Delta E/E \ll 3.3 \cdot 10^{-3}$, a value currently achievable at SPARC. The diffusion velocity in the longitudinal phase space can be deduced by fig. 3 where the quantity $\langle\Delta\gamma^2\rangle = E_{\mathrm{rms}}^2/(mc^2)^2$ is reported as a function of Δt, in the absence and in the presence of laser diffraction.

The slope of the curve $\mathrm{d}\langle\gamma^2\rangle/\mathrm{d}(\Delta t)$ can be evaluated, in the case without diffraction, by means of numerical evidence and is about 0.27. In the realistic case with the presence of diffraction, $\mathrm{d}\langle\gamma^2\rangle/\mathrm{d}(\Delta t)$ tends to zero.

The parameters of the second calculation were chosen in the range of those of the European Proposal for the γ-source ELI-NP [13], and are summarized in table 1, column (B). The diffraction of the laser beam has been disregarded.

Despite the fact that the emitted photon energy value is ten times larger than the preceding case, the phenomenon is quite similar, as shown in fig. 4. The formation of stripes can be observed, that first fill up and then release electrons toward lower energies by cascaded emission of photons. The distribution slowly evolves toward a smoother and smoother function, and tends to the Rayleigh distribution when F_X approaches 1.

Finally we will show a calculation made with a realistic electron and with laser beams simulated with the codes PARMELA [20] and ELEGANT [21] for the case of ELI-NP, whose parameters are presented in table 1, column (C).

The electron beam has been generated from a photo-injector similar to SPARC [12] and transported along the ELI linac [13]. A particular care has been attributed to the control of the energy spread and of the emittance of the electrons, the beam used being the result of a tight optimization with respect to its brightness. The parameters of the electron beam at the first interaction point foreseen in ELI-NP are described in table 1, column (C) together with those of the laser, which is supposed to be a Nd:Yb operating at 500 nm. The laser and electron beam are matched in the interaction area ($\sigma_e \approx \sigma$) and the diffraction of the laser beam has been taken into account.

The energy spread ΔE of the electron beam is rather low, so it leads to a factor $\hbar\omega/\Delta E \approx 20$, which does not affect the formation of the stripes.

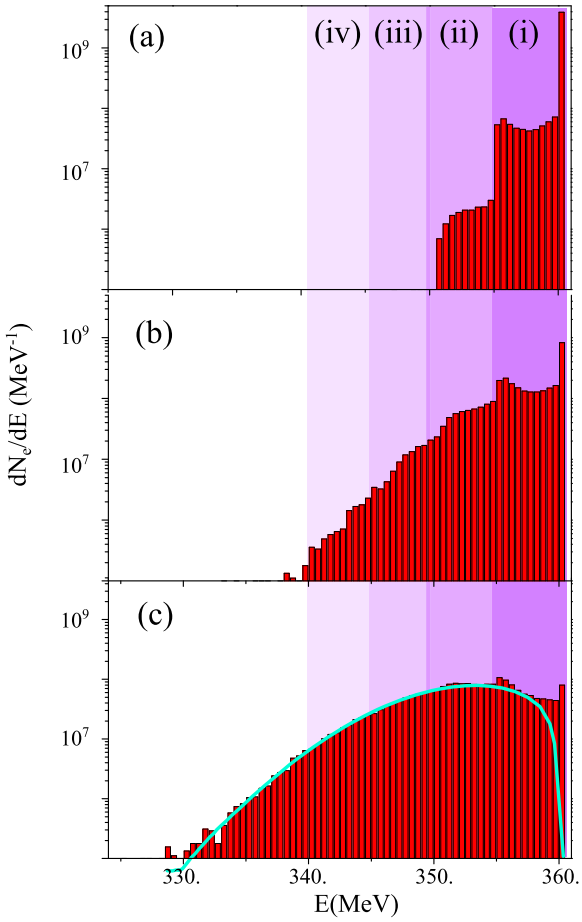

Fig. 4: (Colour on-line) Electron distribution $\mathrm{d}N_e/\mathrm{d}E$ (MeV^{-1}) *vs.* electron energy in MeV for $a_0 = 0.046$: (a) $\Delta t = 0.33$ ps, $E_L = 2$ J ($F_X = 0.027$); (b) $\Delta t = 3.33$ ps, $E_L = 20$ J ($F_X = 0.27$); (c) $\Delta t = 8.32$ ps, $E_L = 50$ J ($F_X = 0.68$). The curve in panel (c) represents the Rayleigh distribution function associated to random walk for $N = 4$.

Figure 5(B) displays, on the other hand, the detail of the photon energy spectrum near the Compton edge, showing that no photons are emitted above 4.82 MeV.

The effect of a sequence of collimators set on the trajectory of the emitted photons is also presented in this same figure. They permit to select the radiation after the emission, intercepting only those photons traveling on axis. As a consequence of the angular-frequency correlation, only part of the spectrum is collected, providing radiation with thin relative bandwidth, of the order of 10^{-3}, a value suitable for nuclear physics and applications. The electron energy distribution after the collision is presented in fig. 6 on two different scales, together with the initial one at the interaction point. It has to be noted that a realistic length of the laser of 5 ps, with an energy of 1 J, leads to a rather low value of the parameter $F_X \approx 0.021$.

Despite the fact that the principal effect observed is a slight drift of the peak toward lower values due to the emission of photons out of axis with energy lower than the nominal resonance value (fig. 6(A)), the presence of the tail toward the low-energy side appears visible

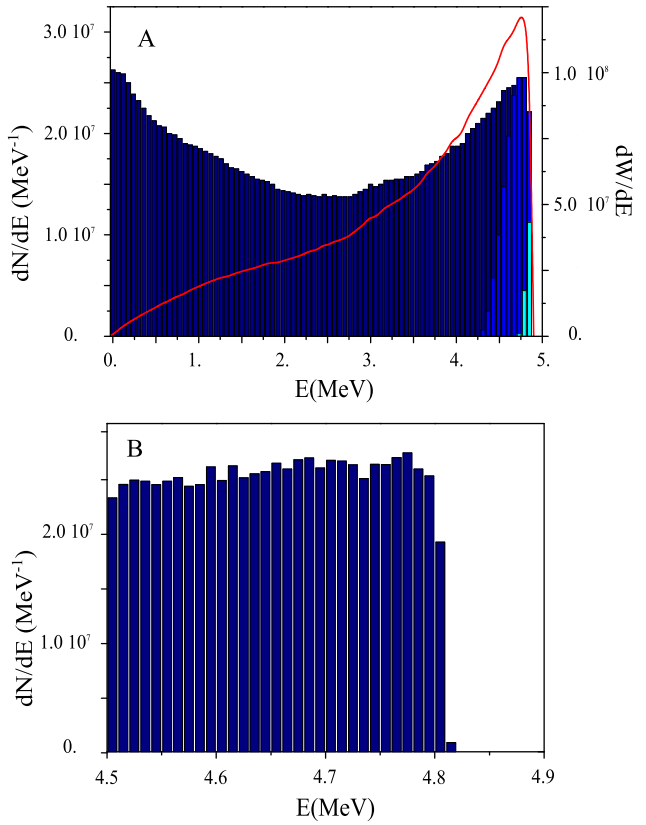

Fig. 5: (Colour on-line) Spectrum of the photons emitted after the collision for the parameters of table 1. Statistics made with $2.5 \cdot 10^6$ macro particles (corresponding to $1.56 \cdot 10^9$ real electrons). Number of macro γ photons generated: $1.41 \cdot 10^6$ ($8.847 \cdot 10^7$ γ real photons). (A) On the left axis: navy columns: complete spectrum without collimators; blue columns: one collimator; cyan columns: two collimators. On the right axis: red line: energy spectrum of the radiation. (B) Detail of the photon energy distribution near the Compton edge, showing that no photons are emitted with energy larger than 4.82 MeV.

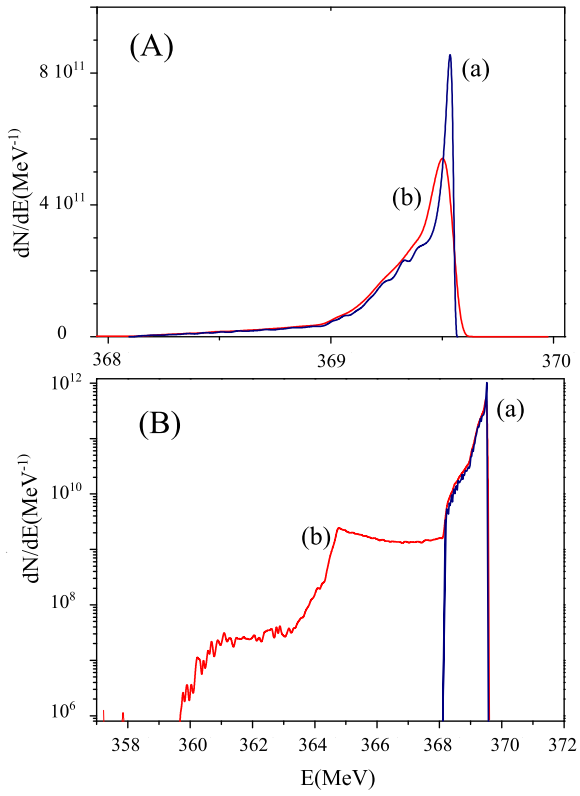

Fig. 6: (Colour on-line) A) Electron energy spectrum $\mathrm{d}N/\mathrm{d}E(\mathrm{MeV}^{-1})$ *vs.* E (MeV) for the same parameters as in fig. 5. Curve (a): before the interaction. Curve (b): after the interaction. (B) Same as (A), but on logarithmic scale, that permits to see the distribution tail.

when the ordinate is converted to logarithmic scale, and is shaped as a sequence of degrading plateaus. As already discussed, the first of them between 368 MeV and 364.5 MeV has a specular shape with respect to the photon spectrum, the second below 364 MeV begins to present numerical noise, which becomes dominant below 360 MeV. The electrons with larger initial energy, by scattering photons of 4.9 MeV on axis, create the flat secondary peak at 365 MeV, while the plateau between 369.5 MeV and 365 MeV is due to the off-axis emission. The bump between 365 MeV and 360 MeV reveals the occurrence of cascaded emission. Since no photons are emitted with energy larger than 4.82 MeV, as confirmed in fig. 5(B), this secondary emission is surely due to electrons that emit two or more photons in sequence. As a consequence of the diffusion and of the formation of the tail, the r.m.s. electron energy bandwidth increases from the initial value of 0.23 MeV to 0.4 MeV.

In conclusion, the evolution of the phase space has been studied by means of numerical calculation based on the code CAIN. The results lead to the conclusion that, in the regime considered, the initial effect is the formation of stripes, due to modeling of the scattering as a two-point-particle collision between an electron and a photon. In the following, when the electrons undergo more collisions, a regime of diffusion of the more energetic particles toward lower values in the longitudinal phase space takes place. The longitudinal phase space of the electrons does not obey a simple finite-difference equation as proposed in [1], but a more general model, based on the master equation derived from the Chapman-Kolmogorov equation for Markov phenomena with a suitable transition probability, must be adopted, as shown in [8]. A measurement of the electron distribution after the scattering might therefore help in having insight into the nature of the collision.

* * *

The authors gratefully thank C. Maroli, L. Giannessi, M. Quattromini, J. Rau, G. Dattoli for continuous interest and stimulating and fruitful discussions, as well as G. Robb and Prof. R. Bonifacio, despite their different opinions on the argument.

REFERENCES

[1] Robb G. R. M. and Bonifacio R., *EPL*, **94** (2011) 34002.

[2] Robb G. R. M. and Bonifacio R., *Phys. Plasmas*, **19** (2012) 073101.
[3] Saldin E. J., Schneidmiller E. A. and Yurkov M. V., *Nucl. Instrum. Methods Phys. Res. A*, **381** (1996) 545.
[4] Benson S. and Madey J. M. J., *Nucl. Instrum. Methods Phys. Res. A*, **237** (1985) 55.
[5] Geloni G., Kocharyan V. and Saldin E., *EPL*, **98** (2012) 44001.
[6] Geloni G., Kocharyan V. and Saldin E., DESY Report 12-022, *On quantum effects in spontaneous emission by a relativistic electron beam in an undulator*, `http://arxiv.org/abs/1202.0691` (2012) 44001.
[7] Potylitsyn A. and Kol'chuzhkin A., *EPL*, **100** (2012) 24006.
[8] Kol'chuzhkin A. *et al.*, *Nucl. Instrum. Methods Phys. Res. B*, **201** (2003) 307.
[9] Yokoya K., KEK report 85-9, 6 October (1985).
[10] CAIN, `http://www-acc-theory.kek.jp/members/cain` (1985).
[11] Oliva P., Bacci A., Bottigli U., Carpinelli M., Delogu P., Ferrario M., Giulietti D., Golosio B., Petrillo V. and Serafini L. *et al.*, *Nucl. Instrum. Methods Phys. Res. A*, **615** (2010) 93.
[12] Giannessi L. *et al.*, *Phys. Rev. ST Accel. Beams*, **14** (2011) 060712.
[13] European proposal for the Compton gamma-ray of ELI-NP, `www.e-gammas.com`.
[14] Blumenthal G. and Gould R., *Rev. Mod. Phys.*, **42** (1970) 237.
[15] Sun C. and Wu Y. K., *Phys. Rev. ST Accel. Beams*, **14** (2011) 044701.
[16] Petrillo V. *et al.*, *Nucl. Instrum. Methods Phys. Res. A*, **693** (2012) 109.
[17] Gizzi L., Bacci A. and Betti S. *et al.*, *Eur. Phys. J. ST*, **175** (2009) 3.
[18] Hartemann F. V., Brown W. J., Gibson D. J., Anderson S. G., Tremaine A. M., Springer P. T., Wootton A. J., Hartouni E. P. and Barty C. P. J., *Phys. Rev. ST Accel. Beams*, **8** (2005) 100702.
[19] Tomassini P. *et al.*, *IEEE Trans. Plasma Sci.*, **36** (2008) 1782.
[20] Young L. M., *PARMELA*, Los Alamos National Laboratory report LA-UR-96-1835 (revised, April 22, 2003).
[21] Borland M., *elegant: A Flexible SDDS-Compliant Code for Accelerator Simulation*, Advanced Photon Source LS-287, September 2000.